Case Study of Phase Transition in Cellular Models of Pedestrian Flow

Marek Bukáček[1,⋆] and Pavel Hrabák[1,2]

[1] Faculty of Nuclear Sciences and Physical Engineering
Czech Technical University in Prague
Trojanova 13, 120 00 Prague, Czech Republic
{bukacma2,pavel.hrabak}@fjfi.cvut.cz
[2] Institute of Information Theory and Automation
Academy of Sciences of the Czech Republic
Pod Vodarenskou vezi 4, 182 08 Prague, Czech Republic
hrabak@utia.cas.cz

Abstract. One room with one exit and one multiple entrance is modelled using 32 different settings and modifications of floor field model. The influence of following aspects are investigated in the scope of the transition from free flow to congestion phase with respect to the inflow rate: Heterogeneity/Homogeneity; With/Without bounds; Moore/von Neumann neighbourhood; Synchronous/Asynchronous update; High/Low friction. Considering the average travel time through the room and average room occupancy the settings incorporating the bounds and synchronous update seems to match the experimental data from the qualitative point of view.

Keywords: Floor field model, phase transition, travel time, bounds principle, asynchronous update.

1 Introduction

Cellular automata models are very useful tool for real time simulations of egress or evacuation of large and complex facilities [12]. Such network consists of several connected segments with exits and entrances.

Cellular models investigated in this article are based on the floor field model described in [8]. Our aim is to investigate the influence of several aspects that modify the FF model. Basic overview of floor field model modifications can be found in [9], [10], [11]. We focus on the modifications leading to real microscopic behaviour as line formation or heterogeneity of agents as mentioned in [1] or [6].

Different approaches are compared within the scope of phase transition in simple design of one room with one exit and one multiple entrance, which could be considered as one segment of larger network. In [4] or [5] the transition from low to high density with respect to inflow parameter α has been studied for simple floor field model.

⋆ Corresponding author.

J. Wąs, G.C. Sirakoulis, and S. Bandini (Eds.): ACRI 2014, LNCS 8751, pp. 508–517, 2014.

The inflow rate α determines the number of pedestrians willing to enter the room during 1 s. General feature of similar hopping particle systems with open boundaries is an existence of a critical (saturation) inflow α_S indicating phase transition. Similarly to [4], we aim to study the boundary induces phase transition between the free flow phase (characterized by the low density) and the congested phase (high density) in the dependence on inflow α. Considered modification of FF model are investigated in the steady state.

2 Considered Models

As mentioned above, we focus on the simulation of passing through a room with the entrance on one side and the exit on the opposite side. To match the experiments described in [1] and [2], the room was equipped with one exit of the width corresponding to one cell and three entrances placed on the opposite wall to the exit, as illustrated in Figure 1. The inflow is controlled by the inflow parameter α, which determines the number of pedestrians coming to the entrance per one second (i.e., if the room capacity is reached, agents are accumulated in front of the entrance). For purposes of the simulation, the room 7.2 m long and 4.4 m wide has been chosen. The cellular model used for the simulation is described below.

Commonly, the space is divided into square cells by rectangular lattice $\mathbb{L}$ with lattice constant equal to 0.4 m. Every cell is denoted by the position of it's center $x = (x_1, x_2)$, the scale of axes x_i corresponds to the lattice constant. The exit is placed to the origin $E = (0, 0)$. As we consider a simple rectangular room, the "playground" is given by cells $x \in \{-w, -w+1, \ldots, w-1, w\} \times \{1, 2, \ldots, l\} \cup \{E, I_{-1}, I_0, I_1\}$, where $2w+1$ is the width and l is the length of the room in cells, i.e., $w = 5$ and $l = 18$ for above described setting; $I_j = (j, l+1)$ are the cells of the entrances, as illustrated in Figure 1.

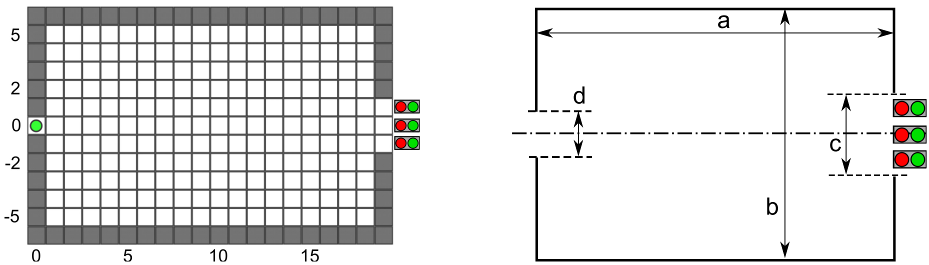

Fig. 1. The room with parameters $a = 7.2$ m, $b = 4.4$ m, $c = 1.3$ m, $d = 0.5$ m is modelled by the rectangular lattice 11×18 cells, i.e., $w = 5$, $l = 18$

Every cell can be either occupied by one agent (representing the pedestrian) or empty. In the following, this is captured by the occupation identifier O, i.e., $O(y) = 1$ for occupied cell and $O(y) = 0$ for the empty cell, $y \in \mathbb{L}$. As we will often evaluate the occupancy of the cells from the point of view of the agent sitting in cell x, it is beneficial to use the "personal" occupancy identifier $O_x(y)$ with $O_x(x) = 0$ and $O_x(y) = O(y)$ for $y \neq x$. This is useful for the agent not to block it's actual cell during the decision process.

To simulate and control the randomized inflow of pedestrians into the room, geometric distribution was used. The number of steps between the input of two consecutive agents to one entrance I_j is given stochastically by the geometric distribution, i.e., the probability of another agent coming to the row in front of the entrance I_j is

$$p(k) = (\alpha h/3)(1 - \alpha h/3)^{k-1}\,, \tag{1}$$

where h is the length of the algorithm step, which depends on the used updating scheme, as described below.

2.1 Decision Process

Agents (pedestrians) are moving along the lattice by hopping from one cell to another. For purposes of this article the nearest-neighbour interaction has been chosen, i.e., the agent is choosing only cells in the nearest neighbourhood. More precisely, an agent in the cell x can choose to jump to the cell $y \in N(x)$, where

$$N(x) = \left\{ y \in \mathbb{L};\ \max_{j=1,2} |x_j - y_j| \leq 1 \right\} \tag{2}$$

is the Moore neighbourhood of the cell x. To distinguish the diagonal and non diagonal motion the diagonal direction indicator D is used in this article, i.e., $D_x(y) = 1$ if $(x_1 - y_1) \cdot (x_2 - y_2) \neq 0$ and $D_x(y) = 0$ otherwise.

The main advantage of the floor-field model is the incorporation of the static field S that is closely related to the distance of the cell to the exit and therefore indicates the cell atractivity (shorter distance to the exit means grater benefit for the particle when hopping to the cell). In our case the value $S(y)$ is the euclidean distance of the cell centre to the exit

$$S(y) = \left(|y_1|^2 + |y_2|^2\right)^{1/2}\,. \tag{3}$$

As usual, the parameter connected to the field F is denoted by k_F.

The crucial idea of the floor-field model is the probabilistic decision process of choosing the target cell. An agent sitting in cell x chooses it's next target cell according to the probability

$$P(x \to y) = \frac{1}{\mathcal{N}} \exp\big\{ - k_S S(y) \big\} \big(1 - k_O O_x(y)\big)\big(1 - k_D D_x(y)\big)\,. \tag{4}$$

The normalization $\mathcal{N}$ assures that $\sum_{y \in N(x)} P(x \to y) = 1$, parameters k_O and k_D are used to distinguish different settings of this general model. The parameter k_S has been set to the value $k_S = 3.5$ to balance the deterministic motion in free flow and stochastic behaviour in the congested cluster (see [1] or [6]). As will be explained in detail below, for purposes of this article two values of k_O

have been chosen: $k_O = 1$ corresponding to the situation that occupied cells are excluded from the decision process and $k_O = 0$ incorporating the possibility of choosing an occupied cell, which is closely related to the principle of bounds. Analogically, $k_D = 1$ corresponds to the von Neumann neighbourhood and $k_D = 0.7$ corresponds to the Moore neighbourhood with certain diagonal movement penalisation [6].

2.2 Asynchronous Update

Aside the decision process, the case study focuses on the influence of updating scheme. Updating schemes presented in this article are inspired by the asynchronous cellular automata schemes presented in [3]. We use similar approach to the *clocked* scheme, i.e., every agent has assigned it's own timer which ticks at different rates for different agents. Furthermore, when the principle of bounds is incorporated ($k_O = 1$), the timer is influenced by the motion of other agents, as will be mentioned below and is discussed in [1].

If we denote by τ_α own period of the agent $\alpha \in A$, the time of agent's next activation is calculated as $t_{\text{next}} = t_{\text{actual}} + \tau_\alpha$. For the study here two cases are distinguished: homogeneous and heterogeneous. In the homogeneous case, all agents have the same own period $\tau = 0.3$ s (1.33 ms^{-1} in free flow); in heterogeneous case two kinds of agents are considered: faster agents with $\tau_1 = 0.3$ s and slower agents with $\tau_2 = 0.4$ s (1.00 ms^{-1} in free flow) with the ratio of occurrence 50 %.

To distinguish the synchronous and asynchronous update within the heterogeneous case, the time-line has been divided into isochronous intervals of the length $h > 0$. Within the k-th step of the algorithm, such agents are activated, whose time of next activation t_{next} belongs to the interval $\langle kh; (k+1)h)$. The value of $h = 0.3$ s corresponds to the synchronous update (slower agents "miss" one of four steps) and $h = 0.05$ corresponds to the asynchronous update.

To compensate the length of the diagonal step in the case of Moore neighbourhood, which is $\sqrt{2}$-times longer, the next activation time after such step is calculated as $t_{\text{next}} = t_{\text{actual}} + \tau_\alpha \cdot q$, where q is a rational approximation of $\sqrt{2}$ in this article chosen to be $q = 3/2$. This is together with the bounds principle called *adaptive time span* [1].

2.3 Bounds and Conflicts

The bounds principle is closely related to the possibility of choosing an occupied cell ($k_O \neq 1$). If an agent chooses as his target cell an occupied cell then the *bound* to the blocking agent is created. The bound holds until the blocker moves or until the blocked agent is activated. In the case of the earlier movement of the blocker (i.e., if the blocker moves within the algorithm step before the activation of the blocked agent), the blocked agent follows the blocking agent immediately outside his activation step. This principal supports the motion in lines and is further discussed in [1] or [6].

In this article simple solution of conflicts using the friction parameter μ investigated in [7] is used. If more agents try to enter the unoccupied cell, with probability μ none of the agents moves; with probability $1 - \mu$, of the agents is chosen at random to enter the cell. Other agents remain in their original cells. Analogically is the conflict solved in the case, when more then one agent is bounded to common blocking agent.

3 Phase Transition in Simulations

In [4] the transition from low density to high density phase in dependence on inflow parameter α has been investigated with respect to the friction function parameter ζ. In this article we focus on such dependence on the model type classified according to Table 1. The investigation is far from complete parameter investigation or validation. We aim above all to point out characteristic features and mechanism of the transition.

As we aim to investigate the system in the steady state, we have let the model to evolve for a long period. By the free flow setting we understand such set of parameters under which the room does not become overfilled by the agents. The congested setting is characterized by the creation of stable cluster in front of the exit, which size grows to the capacity of the room. By the transition from the free flow to the congestion phase we understand the change from free flow to congestion setting by increasing inflow parameter α.

We distinguish 32 combinations of different representative settings according to Heterogeneity/Homogeneity; With/Without bounds; Moore/von Neumann neighbourhood; Synchronous/Asynchronous update; High/Low friction. The numbering of given settings together with specific values of parameters is given in Table 1.

Table 1. Numbering of specific settings and given parameters. In the following figures, the setting is identified by the corresponding position as shown in the right part of the table, odd numbers represent high friction. Therefore, setting 11 means heterogeneity, bounds, asynchronous update, Moore neighbourhood, and high friction.

Heterogenous HET: $\tau_1 = 0.3$ s $\tau_2 = 0.4$ s	Homogenous HOM: $\tau = 0.3$ s
No bounds F: $k_D = 1.0$	Bounds O: $k_D = 0.0$
Moore M: $k_O = 0.7$	von Neumann N: $k_D = 1.0$
Synchronous S: $h = 0.3$	Asynchronous A: $h = 0.05$
High friction H: $\mu = 0.7$	Low friction L: $\mu = 0.2$

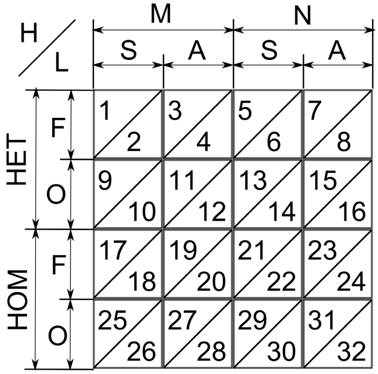

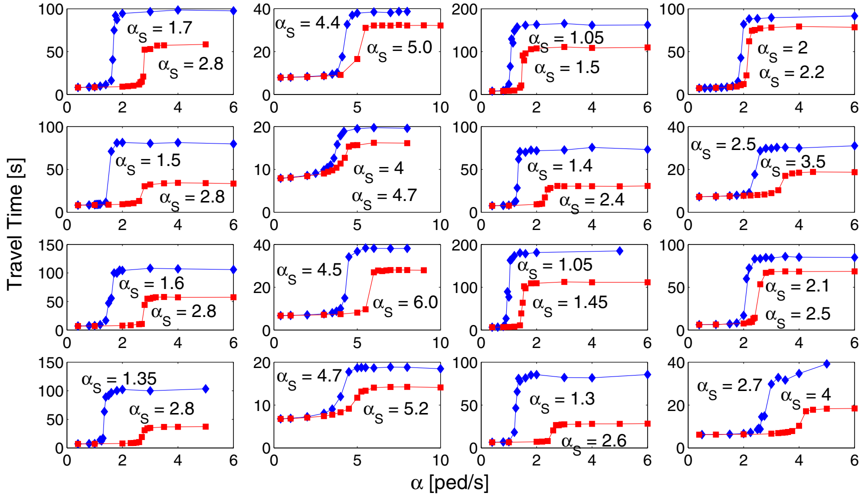

Fig. 2. Travel time with respect to α. The graph position corresponds to Table 1. Blue diamonds represent $\mu = 0.7$ and red squares $\mu = 0.2$.

For each of the 32 settings, simulations with variety of inflow parameters α have been performed. Three basic characteristics have been measured in the steady state: travel time, room occupancy, and real inflow into the room. By the travel time we understand the time an agent spent in the room, i.e., from the time of the entrance (which is different from the time of coming to the row in front of the exit) to the time of leaving the room through the exit; room occupancy denotes the average number of agents inside the room, and the real inflow stands for the number of pedestrians entering the room per second. This quantity corresponds in the steady state to the average flow. Simulation results for dependency of stated quantities are plotted in Figures 2 – 3.

From the Graphs several conclusions can be made:

3.1 Saturation

In Figures 2 – 3, appropriate values of saturation inflow α_S are added to the graphs. From the graphs we can read that the "capacity" of the room is not necessarily close to the number of cells $11 \times 18 = 198$. When the bounds principle is implemented (row 2 and 4, numbers 9-16 and 26-32), the maximal number of pedestrians is significantly lower. This can be explained by the possibility of choosing an occupied cell. Agents partially stand in lines and only several of them are trying to run over the crowd.

3.2 Smooth Transition vs. Sharp Jump

Another important aspect is the shape of the curves near the saturation point. In the majority of the settings the average travel time levels before the saturation

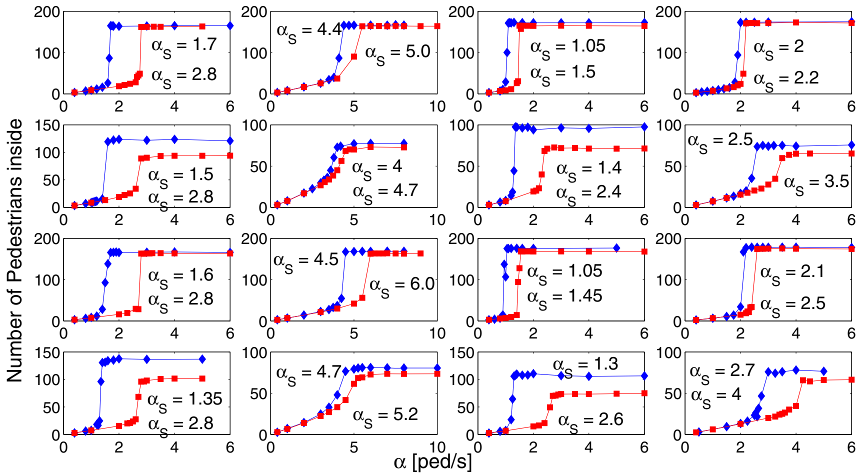

Fig. 3. Occupancy with respect to α. The graph position corresponds to Table 1. Blue diamonds represent $\mu = 0.7$ and red squares $\mu = 0.2$.

point (number of pedestrians increases linearly). The change of the curves towards the saturation value is sharp, jump-like. In settings with bounds and asynchronous updates (numbers 11/12, 15/16, 27/28, and 31/32) is the transition much smoother with respect to inflow α. The Travel time increases slightly before the saturation point and smoothly reaches the maximum corresponding to the saturation. This phenomenon is more obvious in the case of Moore neighbourhood (columns 1 and 2), as expected. the smooth shape of the travel time curve in the case of bounds can be explained by the motion in lines which is supported by this principle. Agents are rather waiting in lines then walk around each other. In the higher inflow case $(2.0 < \alpha < 4.0)$ leads to slight increase of the travel time, but suppresses the overall delay caused by the friction.

3.3 Heterogeneous vs. Homogeneous

From the observations it follows that the heterogeneity of the system does not qualitatively nor quantitatively influence the system on the macroscopic bases captured by the travel time, occupancy, or saturation point. This is mainly caused by two aspects. Firstly, the macroscopic quantities are compared by means of aggregated data, which suppresses the heterogeneity nature. Secondly, the heterogeneity in the setting is given by the 50-50 distribution of velocities τ_1 and τ_2 keeping the decision process intact (there are no aggressive pedestrians etc.). Nevertheless, in microscopic point of view does the heterogeneity influence the histograms of travel time in the free flow with $\alpha \ll \alpha_S$ as shown in Figure 4.

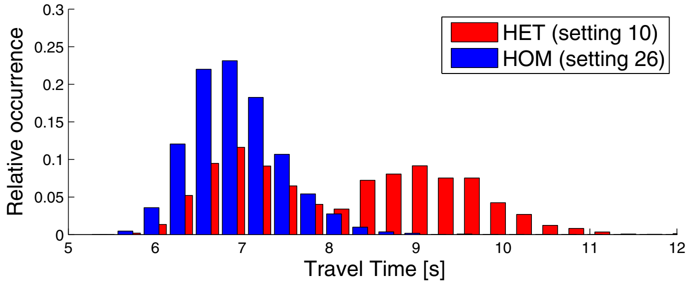

Fig. 4. Travel time histograms for free flow $\alpha = 0.4$ ped/s

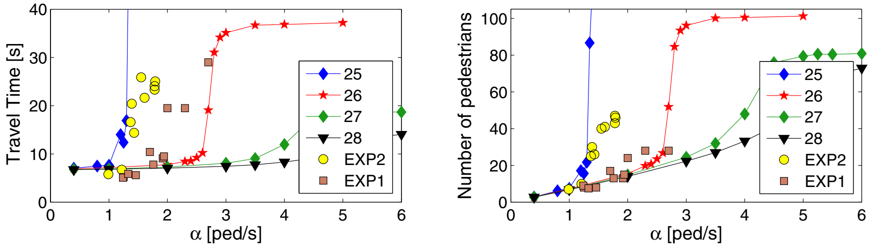

Fig. 5. Comparison of selected settings with experiments (yellow circles and orange squares)

3.4 The Friction Parameter μ

The friction parameter influences mainly the behaviour of the system with synchronous updates. Although the value $\mu = 0.7$ seems to be unrealistic (values between 0.2 and 0.3 are commonly used as e.g. in [7]), in the settings incorporating bounds and/or asynchronous update the number of conflicts is suppressed, therefore it is important to increase the friction to maintain the ratio of conflicts per time unit.

3.5 Comparison with Experiments

Our research group organized several experiments with similar setting to the simulations described in this article. Those experiments were designed to observe the phase transition by means of stability of the cluster in front of the exit. The discussion concerning mentioned experiment can (or will) be found in [1] and [2]. Additional experiment was organized in 29th April 2014. Similarly to previous experiments, 80 volunteers from FNSPE CTU were walking through the experimental room. As the number of volunteers did not reach the capacity of the room, the numbers of pedestrians in the room as well as the average travel time measured was lower then in appropriate steady state. Therefore, the congestion phase was recognized by means of growing number of pedestrians in the room.

In Figure 5 four representatives are compared with two sets of experimental data. In agreement with [1], the transition from free flow to stable cluster was observed at inflow rate $\alpha \in (1.3, 1.6)$ ped/s (Compare to J_{in} of Table 2 in [1]). Here we note that the setting 25 is similar to the model presented there.

4 Conclusion

To conclude the previous section, it is obvious and expected that different settings and modifications of floor field model significantly influence the macroscopic behaviour of the system. In this article qualitative analyses of different approaches has been performed by means of the phase transition from low to high density with respect to the inflow parameter α.

Three characteristics have been used as the indicator of the saturation point and shape of the transition: average travel time, average occupancy of the room and average inflow. The analyses of the settings 11/12, 15/16, 27/28, and 31/32 (bounds and asynchronous update) shows that the transition does not have to be sharp and jump-like. In the mentioned settings the transition is rather smooth with respect to the inflow α.

From the evaluation of experiments it follows that setting with higher friction does better correspond to the identified saturation point $\alpha_S \approx 1.4$ ped/s when principle of bounds is implemented. Furthermore, the synchronous update leads to better correspondence as well, as can be shown in Figure 5, where synchronous settings 25/26 are compared to asynchronous settings 27/28. The asynchronous update significantly suppresses the conflicts and therefore increases the maximal outflow from the room which leads to unrealistic high value of the saturation $\alpha \approx 4$ ped/s.

From the above mentioned analysis supported by the simple observation of the microscopic motion we conclude that the synchronous update with bounds, high friction, and Moore neighbourhood is in the best correspondence with performed experiments.

Acknowledgements. This work was supported by the grant SGS12/197/OHK4/3T/14 and by the Czech Science Foundation under the grant 13-13502S. We would like to thank Mr. Milan Krbálek and his students for assistance in mentioned experiments.

References

1. Bukáček, M., Hrabák, P., Krbálek, M.: Cellular model of pedestrian dynamics with adaptive time span. In: Wyrzykowski, R., Dongarra, J., Karczewski, K., Waśniewski, J. (eds.) PPAM 2013, Part II. LNCS, vol. 8385, pp. 669–678. Springer, Heidelberg (2014)
2. Bukáček, M., Hrabák, P., Krbálek, M.: Experimental analysis of two-dimensional pedestrian flow in front of the bottleneck. In: Traffic and Granular Flow 2013. Springer, Heidelberg (to be published, 2014)

3. Cornforth, D., Green, D.G., Newth, D.: Ordered asynchronous processes in multi-agent systems. Physica D 204(1-2), 70–82 (2005)
4. Ezaki, T., Yanagisawa, D., Nishinari, K.: Analysis on a single segment of evacuation network. Journal of Cellular Automata 8(5-6), 347–359 (2013)
5. Ezaki, T., Yanagisawa, D., Ohtsuka, K., Nishinari, K.: Simulation of space acquisition process of pedestrians using proxemic floor field model. Physica A 391(1-2), 291–299 (2012)
6. Hrabák, P., Bukáček, M., Krbálek, M.: Cellular model of room evacuation based on occupancy and movement prediction: Comparison with experimental study. Journal of Cellular Automata 8(5-6), 383–393 (2013)
7. Kirchner, A., Nishinari, K., Schadschneider, A.: Friction effects and clogging in a cellular automaton model for pedestrian dynamics. Physical Review E 67(5 2), 056122/1–056122/10 (2003)
8. Kirchner, A., Schadschneider, A.: Simulation of evacuation processes using a bionics-inspired cellular automaton model for pedestrian dynamics. Physica A: Statistical Mechanics and its Applications 312(1-2), 260–276 (2002)
9. Nishinari, K., Kirchner, A., Namazi, A., Schadschneider, A.: Simulations of evacuation by an extended floor field ca model. In: Hoogendoorn, S., Luding, S., Bovy, P., Schreckenberg, M., Wolf, D. (eds.) Traffic and Granular Flow 2003, pp. 405–410. Springer, Heidelberg (2005)
10. Schadschneider, A., Chowdhury, D., Nishinari, K.: Stochastic Transport in Complex Systems: From Molecules to Vehicles. Elsevier Science B. V., Amsterdam (2010)
11. Schadschneider, A., Seyfried, A.: Empirical results for pedestrian dynamics and their implications for cellular automata models. In: Timmermans, H. (ed.) Pedestrian Behavior - Models, Data Collection and Applications, pp. 27–43. Emerald Group, Bingley (2009)
12. Was, J., Lubaś, R.: Adapting social distances model for mass evacuation simulation. Journal of Cellular Automata 8(5-6), 395–405 (2013)